

iments, low dose/low-dose rate γ -irradiation (30 mGy at 1.2 mGy/h) did not significantly affect end joining (EJ) repair of this specific DSB, but it enhanced the efficiency of HR repair by about 50% (unpublished data). The small homozygous LOH events we observed in the primed cells in the present study (3/14) might reflect this enhanced HR, but we must examine whether the adaptive response was really involved because we also recovered small homozygous LOH mutants after the low-dose/low-dose rate γ -ray exposures [32]. The decrease in the frequency of single-base substitutions that we observed in primed cells (1/48) versus non-primed cells (7/46) (Tables 4 and 5) is rarely influenced by counting base substitutions accompanied by single base deletions (which would result in 2/48 for primed cells and 9/46 for non-primed cells), so the most likely mechanism for the reduced induction of non-LOH mutants was suppression of base substitutions.

One of the possible targets for radioadaptation is oxidative base damage. In fact, down-regulation of the human *CDC16* gene that occurs after oxidative stress causes more rapid and efficient repair in adapted (2 cGy pre-irradiated) human lymphoblastoid cells challenged with 4 Gy irradiation [6]. On the other hand, oxidative base excision repair enzymes, including DNA glycosylases, hOGG1 and hNth1, are reportedly not up-regulated at the post-transcriptional level in γ -ray-primed TK6 cells [33]. Since DNA glycosylase can suppress base substitution, we need to examine whether radioadaptation enhances the enzyme's activity under the present condition. Alternatively, base substitution activity might not accurately reflect DNA glycosylase activity because attempted base excision repair of IR damage by the enzyme can lead to lethal and mutagenic DSBs [34].

A variety of untargeted effects may contribute to the short- and long-term fate of a cell exposed to IR [35]. An example is the possible involvement of a "radioadaptive bystander" effect in human lung fibroblasts [36]. The reduction of radiosensitivity in cells with a wild type *p53* gene by a radiation-induced, nitric oxide (NO)-mediated bystander effects may be a manifestation of the radioadaptive response [37,38]. This possibility is supported by the finding that the NO-induced apoptosis observed in lymphoblastoid and fibroblast cells depends on the phosphorylation and activation of *p53* [39]. However, it is still unclear whether the NO-mediated pathway also contributes to the mutagenic adaptation. The de novo protein synthesis is required for expression of adaptive responses [22,40], and gene expression studies are improving our understanding of the molecular mechanisms underlying the radioadaptive response [9,10,40,41]. Our laboratory is also focusing on the molecular mechanisms involved

in radioadaptation, especially the expression of genes involved in DNA base and nucleotide excision repair.

Acknowledgements

This study was partially supported by the Budget for Nuclear Research of the Ministry of Education, Culture, Sports, Science and Technology, and was reviewed by the Atomic Energy Commission of Japan. We thank Dr. Miriam Bloom (SciWrite Biomedical Writing & Editing Services) for professional editing.

References

- [1] G. Olivieri, Y. Bodycote, S. Wolf, Adaptive response of human lymphocytes to low concentrations of radioactive thymidine, *Science* 223 (1984) 594–597.
- [2] S. Wolf, Aspects of the adaptive response to very low doses of radiation and other agents, *Mutat. Res.* 358 (1996) 135–142.
- [3] S. Wolf, The adaptive response in radiobiology: evolving insights and implications, *Environ. Health Perspect.* 106 (1998) 277–283.
- [4] O. Rigaud, E. Moustacchi, Radioadaptation for gene mutation and the possible molecular mechanisms of the adaptive response, *Mutat. Res.* 358 (1996) 127–134.
- [5] M. Wojewodka, M. Kruzewski, K. Iwanenko, I. Szumiel, Effects of signal transduction in adapted lymphocytes: micronuclei frequency and DNA repair, *Int. J. Radiat. Biol.* 71 (1997) 245–252.
- [6] P.-K. Zhou, O. Rigaud, Down-regulation of the human *CDC16* gene after exposure to ionizing radiation: a possible role in the radioadaptive response, *Radiat. Res.* 155 (2001) 43–49.
- [7] M.S. Sasaki, Y. Ejima, A. Tachibana, T. Yamada, K. Ishizaki, T. Shimizu, T. Nomura, DNA damage response pathway in radioadaptive response, *Mutat. Res.* 504 (2002) 101–118.
- [8] I. Szumiel, Adaptive responses: stimulated DNA repair or decreased damage fixation? *Int. J. Radiat. Biol.* 81 (2005) 233–241.
- [9] M.A. Coleman, E. Yin, L.E. Peterson, D. Nelson, K. Sorensen, J.D. Tucker, A.J. Wyrobeck, Low-dose irradiation alters the transcript profiles of human lymphoblastoid cells inducing genes associated with radioadaptive response, *Radiat. Res.* 164 (2005) 369–382.
- [10] H.P. Wang, X.H. Long, Z.Z. Sun, O. Rigaud, Q.Z. Xu, Y.C. Huang, J.L. Sui, B. Bai, P.K. Zhou, Identification of differentially transcribed genes in human lymphoblastoid cells irradiated with 0.5 Gy of γ -ray and the involvement of low dose radiation inducible *CHD6* gene in cell proliferation and radiosensitivity, *Int. J. Radiat. Biol.* 82 (2006) 181–190.
- [11] S.G. Swant, G. Randers-Pehrson, N.F. Metting, E.J. Hall, Adaptive response and the bystander effect induced by radiation in C3H 10T1/2 cells in culture, *Radiat. Res.* 156 (2001) 177–180.
- [12] H.N. Zhou, G. Randers-Pehrson, C.R. Geard, D.J. Brenner, E.J. Hall, T.K. Hei, Interaction between radiation-induced adaptive response and bystander mutagenesis in mammalian cells, *Radiat. Res.* 160 (2003) 512–516.
- [13] W.M. Bonner, Thresholds, bystander effect, and adaptive response, *Proc. Natl. Acad. Sci. U.S.A.* 100 (2003) 4973–4975.
- [14] S.A. Mitchell, S.A. Marino, D.J. Brenner, E.J. Hall, Bystander effect and adaptive response in C3H 10T1/2 cells, *Int. J. Radiat. Biol.* 80 (2004) 465–472.

- [15] T.K. Hei, R. Persaud, H. Zhou, M. Suzuki, Genotoxicity in the eyes of bystander cells, *Mutat. Res.* 568 (2004) 111–120.
- [16] T. Ikushima, Chromosomal response to ionizing radiation reminiscent of an adaptive response in cultured Chinese hamster cells, *Mutat. Res.* 180 (1987) 215–221.
- [17] B.J.S. Sanderson, A.A. Morely, Exposure of human lymphocytes to ionizing radiation reduces mutagenicity by subsequent radiation, *Mutat. Res.* 164 (1986) 151–347.
- [18] P.K. Zhou, X.Y. Liu, W.Z. Sun, Y.P. Zhang, Y.P.K. Wei, Cultured mouse SR-1 cells exposed to low-dose of γ -rays become less susceptible to the induction of mutations by radiation as well as bleomycin, *Mutagenesis* 8 (1993) 109–111.
- [19] A.M. Ueno, D.B. Vannais, S.L. Gustafson, J.C. Wong, C.A. Waldren, A low adaptive dose of gamma-rays reduced the number and altered the spectrum of S1 mutants in human hamster hybrid cells, *Mutat. Res.* 358 (1996) 161–169.
- [20] E.I. Azzam, G.P. Raaphorst, R.E. Mitchell, Radiation-induced adaptive response for protection against micronucleus formation and neoplastic transformation in C3H 10T1/2 mouse embryo cells, *Radiat. Res.* 138 (1994) S28–S31.
- [21] O. Rigaud, D. Papadopoulos, E. Moustacchi, Decreased deletion mutation in radioadapted human lymphoblast, *Radiat. Res.* 133 (1993) 94–101.
- [22] T. Ikushima, H. Aritomi, J. Morisita, Radioadaptive response: efficient repair of radiation-induced DNA damage in adapted cells, *Mutat. Res.* 358 (1996) 193–198.
- [23] T.R. Skopek, H.L. Liber, B.W. Penman, W.G. Thilly, Isolation of a human lymphoblastoid line heterozygous at the thymidine kinase locus: possibility for a rapid human cell mutation assay, *Biochem. Biophys. Res. Commun.* 84 (1978) 411–416.
- [24] M. Honma, M. Hayashi, T. Sofuni, Cytotoxic and mutagenic responses to X-rays and chemical mutagens in normal and p53-mutated human lymphoblastoid cell, *Mutat. Res.* 374 (1996) 89–98.
- [25] M. Honma, L.S. Zhang, M. Hayashi, K. Takeshita, Y. Nakagawa, N. Tanaka, T. Sofuni, Illegitimate recombination leading to allelic loss and unbalanced translocation in p53-mutated human lymphoblastoid cells, *Mol. Cell. Biol.* 17 (1997) 4774–4781.
- [26] S. Morimoto, T. Kato, M. Honma, M. Hayashi, F. Hanaoka, F. Yatagai, Detection of genetic alterations induced by low-dose X rays: analysis of loss of heterozygosity for TK mutation in human lymphoblastoid cells, *Radiat. Res.* 157 (2002) 533–538.
- [27] S. Morimoto, M. Honma, F. Yatagai, Sensitive detection of LOH events in a human cell line after C-ion beam exposure, *J. Radiat. Res.* 43 (Suppl.) (2002) S163–S167.
- [28] Y. Umehayashi, M. Honma, T. Abe, H. Ryuto, H. Suzuki, T. Shimazu, N. Ishioka, M. Iwaki, F. Yatagai, Mutation induction after low-dose carbon-ion beam irradiation of frozen human cultured cells, *Biol. Sci. Space* 19 (2005) 237–241.
- [29] F. Yatagai, S. Morimoto, T. Kato, M. Honma, Further characterization of loss of heterozygosity enhanced by p53 abrogation in human lymphoblastoid TK6 cells: disappearance of endpoint hotspots, *Mutat. Res.* 560 (2004) 133–145.
- [30] A.J. Groszky, B.N. Walter, C.R. Giver, DNA-sequence specificity of mutations at the human thymidine kinase locus, *Mutat. Res.* 289 (1993) 231–243.
- [31] M. Honma, M. Izumi, M. Sakuraba, S. Tadokoro, H. Sakamoto, W. Wang, F. Yatagai, M. Hayashi, Deletion, rearrangement, and gene conversion; genetic consequences of chromosomal double-strand breaks in human cells, *Environ. Mol. Mutagen.* 42 (2003) 288–298.
- [32] Y. Umehayashi, M. Honma, M. Suzuki, H. Suzuki, T. Shimazu, N. Ishioka, M. Iwaki, F. Yatagai, Mutation induction in cultured human cells after low-dose and low-dose-rate γ -ray irradiation: detection by LOH analysis, *J. Radiat. Res.* 48 (2006) 7–11.
- [33] M. Inoue, G.-P. Shen, M.A. Chaudhry, H. Galick, J.O. Blaisdell, S.S. Wallace, Expression of the oxidative base excision repair enzymes is not induced in TK6 human lymphoblastoid cells after low doses of ionizing radiation, *Radiat. Res.* 161 (2004) 409–417.
- [34] N. Yang, H. Galick, S.S. Wallace, Attempted base excision repair of ionizing radiation damage in human lymphoblastoid cells produces lethal and mutagenic double-strand breaks, *DNA Repair* 3 (2004) 1323–1334.
- [35] P.J. Coates, S.A. Lorimore, E.G. Wright, Damaging and protective cell signaling in the untargeted effects of ionizing radiation, *Mutat. Res.* 568 (2004) 5–20.
- [36] R. Iyer, B.E. Lehnert, Low-dose, low-LET ionizing radiation-induced radioadaptation and associated early responses in unirradiated cells, *Mutat. Res.* 503 (2002) 1–9.
- [37] H. Matsumoto, A. Takahashi, T. Ohnishi, Radiation-induced adaptive and bystander effects, *Biol. Sci. Space* 18 (2004) 247–254.
- [38] H. Matsumoto, A. Takahashi, T. Ohnishi, Nitric oxide radicals choreograph a radioadaptive response, *Cancer Res.* 67 (2007) 8574–8579.
- [39] L.M. McLaughlin, B. Dimple, Nitric oxide-induced apoptosis in lymphoblastoid and fibroblast cells dependent on the phosphorylation and activation of p53, *Cancer Res.* 65 (2005) 6097–6104.
- [40] J.H. Yongblom, J.K. Wiencke, S. Wolf, Inhibition of the adaptive response of human lymphocytes to very low doses of ionizing radiation by the protein synthesis inhibitor cycloheximide, *Mutat. Res.* 227 (1989) 257–261.
- [41] L.-H. Ding, M. Shingyoji, F. Chen, J.-J. Hwang, S. Burma, C. Lee, J.-F. Chen, D.J. Chen, Gene expression profiles of normal human fibroblasts after exposure to ionizing radiation: a comparative study of low and high doses, *Radiat. Res.* 164 (2005) 17–26.

JMBAvailable online at www.sciencedirect.com

ScienceDirect



Miscoding Properties of 2'-Deoxyinosine, a Nitric Oxide-Derived DNA Adduct, during Translesion Synthesis Catalyzed by Human DNA Polymerases

Manabu Yasui^{1*}, Emi Suenaga², Naoki Koyama¹, Chikahide Masutani³, Fumio Hanaoka³, Petr Gruz¹, Shinya Shibutani⁴, Takehiko Nohmi¹, Makoto Hayashi¹ and Masamitsu Honma¹

¹Division of Genetics and Mutagenesis, National Institute of Health Sciences, 1-18-1 Kamiyoga, Setagaya, Tokyo 158-8501, Japan

²Division of Pharmacogenosy, Phytochemistry and Narcotics, National Institute of Health Sciences, 1-18-1 Kamiyoga, Setagaya, Tokyo 158-8501, Japan

³Cellular Biology Laboratory, Graduate School of Frontier Biosciences, Osaka University, 1-3 Yamada-oka, Suita, Osaka 565-0871, Japan

⁴Department of Pharmacological Sciences, State University of New York at Stony Brook, Stony Brook, NY 11794-8651, USA

Received 26 November 2007;
received in revised form
10 January 2008;
accepted 14 January 2008
Available online
18 January 2008

Edited by J. Karn

Chronic inflammation involving constant generation of nitric oxide ([•]NO) by macrophages has been recognized as a factor related to carcinogenesis. At the site of inflammation, nitrosatively deaminated DNA adducts such as 2'-deoxyinosine (dI) and 2'-deoxyxanthosine are primarily formed by [•]NO and may be associated with the development of cancer. In this study, we explored the miscoding properties of the dI lesion generated by Y-family DNA polymerases (pols) using a new fluorescent method for analyzing translesion synthesis. An oligodeoxynucleotide containing a single dI lesion was used as a template in primer extension reaction catalyzed by human DNA pils to explore the miscoding potential of the dI adduct. Primer extension reaction catalyzed by pol α was slightly retarded prior to the dI adduct site; most of the primers were extended past the lesion. Pol η and pol $\kappa\Delta C$ (a truncated form of pol κ) readily bypassed the dI lesion. The fully extended products were analyzed by using two-phased PAGE to quantify the miscoding frequency and specificity occurring at the lesion site. All pils, that is, pol α , pol η , and pol $\kappa\Delta C$, promoted preferential incorporation of 2'-deoxycytidine monophosphate (dCMP), the wrong base, opposite the dI lesion. Surprisingly, no incorporation of 2'-deoxythymidine monophosphate, the correct base, was observed opposite the lesion. Steady-state kinetic studies with pol α , pol η , and pol $\kappa\Delta C$ indicated that dCMP was preferentially incorporated opposite the dI lesion. These pils bypassed the lesion by incorporating dCMP opposite the lesion and extended past the lesion. These relative bypass frequencies past the dC:dI pair were at least 3 orders of magnitude higher than those for the dT:dI pair. Thus, the dI adduct is a highly miscoding lesion capable of generating A \rightarrow G transition. This [•]NO-induced adduct may play an important role in initiating inflammation-driven carcinogenesis.

© 2008 Elsevier Ltd. All rights reserved.

Keywords: inflammation; nitric oxide; DNA adduct; translesion synthesis; nonradioactive analysis

*Corresponding author. E-mail address: m-yasui@nihs.go.jp.

Abbreviations used: [•]NO, nitric oxide; dI, 2'-deoxyinosine; dX, 2'-deoxyxanthosine; dA, 2'-deoxyadenosine; 8-Oxo-dG, 8-oxo-2'-deoxyguanosine; dNTP, 2'-deoxynucleoside triphosphate; Alexa546, Alexa Fluor 546 dye; pol α , human DNA polymerase α ; pol η , human DNA polymerase η ; pol κ , human DNA polymerase κ ; pol $\kappa\Delta C$, a truncated form of pol κ ; F_{ins} , frequency of insertion; F_{ext} , frequency of extension; 8-NO₂-dG, 8-nitro-2'-deoxyguanosine; dCMP, 2'-deoxycytidine monophosphate; dTMP, 2'-deoxythymidine monophosphate; dTTP, 2'-deoxythymidine triphosphate; dCTP, 2'-deoxycytidine triphosphate; dGTP, 2'-deoxyguanosine triphosphate; Cy3, Cyanin 3; endo V, endonuclease V.

Introduction

Chronic inflammation involving constant generation of nitric oxide ($^{\bullet}\text{NO}$) by macrophages has been recognized as a factor related to carcinogenesis.¹⁻³ $^{\bullet}\text{NO}$ can attack neighboring epithelial and stromal cells by damaging the DNA, altering their genome stability. There are two possible major pathways for the $^{\bullet}\text{NO}$ reaction (Fig. 1). One pathway involves the combination of $^{\bullet}\text{NO}$ and superoxide with the formation of highly toxic peroxynitrite (ONOO^{\bullet}). Spontaneous hydrolysis of peroxynitrite under physiological conditions generates secondary radical species ($^{\bullet}\text{NO}_2$, $^{\bullet}\text{OH}$, and $\text{CO}_3^{\bullet-}$) that induce oxidation and nitration of diverse DNA adducts^{4,5} such as 8-oxo-2'-deoxyguanosine (8-OxodG) and 8-nitro-2'-deoxyguanosine (8- NO_2 -dG).^{6,7} A second involves nitrosative deamination of DNA base by $^{\bullet}\text{NO}$ via formation of several nitrosating agents, which predominantly exist as nitrous anhydride (N_2O_3) at physiological pH.⁸ The DNA base products by nitrosative deamination mainly involve conversion of adenine to hypoxanthine [2'-deoxyinosine (dI)] (Fig. 2), guanine to xanthine [2'-deoxyxanthosine (dX)], and cytosine to uracil.⁹⁻¹²

The spectrum of nitrosative DNA adducts in N_2O_3 -treated plasmid DNA was composed of approximately 2% dG-dG cross-links, 4-6% basic sites, and 25-35% each of dI, dX, and 2'-deoxyuracil.^{12,13} Moreover, dI and dX, as well as lipid peroxidated adducts, were increased in the cellular DNA of tissues from the $^{\bullet}\text{NO}$ -overproducing SJL mouse model of inflammation.¹⁴ The increased production of $^{\bullet}\text{NO}$ was associated with an increased mutation frequency.¹⁵ When human TK6 cells were exposed to $^{\bullet}\text{NO}$, the increase in mutation rates observed at hypoxanthine-guanine



2'-deoxyadenosine (dA)

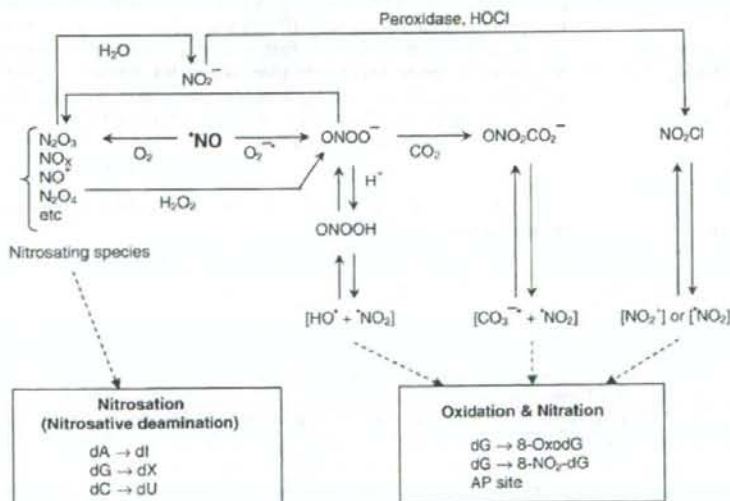
2'-deoxyinosine (dI)

Fig. 2. Structures of dA and dI adducts.

phosphoribosyltransferase and thymidine kinase gene loci correlated with the 40-fold increase of dI and dX more than did that of the controls in the cellular DNA.¹⁰ Thus, the dI adduct is one of the major $^{\bullet}\text{NO}$ -derived DNA lesions and may contribute to the burden of carcinogenesis in inflammation tissue.

Site-specifically dI-modified oligodeoxynucleotides have been used as DNA templates for investigating the miscoding events using only mouse pol α and rat pol β .¹⁶ The previous report showed that rat pol β inserted only 2'-deoxycytidine monophosphate (dCMP) opposite the dI lesion and that mouse pol α tended to incorporate dCMP and 2'-deoxythymidine monophosphate (dTMP) opposite the lesion. However, the miscoding events were investigated with the detection of mismatched base pairs by loss of a restriction enzyme recognition site. No quantitative analysis, therefore, has been performed for determination of miscoding events generated by dI.

Human DNA pol η ¹⁷ and pol κ ^{18,19} that are associated with translesion synthesis past a variety of DNA lesions^{20,21} were examined. We have here explored the miscoding properties of the dI lesion that occurred during DNA replication catalyzed by

Fig. 1. Possible pathways for the formation of $^{\bullet}\text{NO}$ -induced DNA adducts.

human DNA pols. In addition, instead of using radioisotope, we have developed a new fluorescent technique for analyzing translesion synthesis and quantifying the miscoding specificity and frequency using two-phased PAGE (Fig. 3).^{22,23} Relative bypass frequencies past the dI lesion were also determined by steady-state kinetic studies.^{24,25}

Results

Primer extension reactions catalyzed by human DNA pols on dI-modified DNA template

Using unmodified and dI-modified 38-mer templates, we conducted primer extension reactions in the presence of four 2'-deoxynucleoside triphosphates (dNTPs) and varying amounts of pol α , pol η , or pol $\kappa\Delta C$ (Fig. 4). Primer extension occurred rapidly on unmodified templates to form fully extended products. With the dI-modified template, primer extension catalyzed by pol α was slightly retarded one base before the lesion (see arrowhead in Fig. 4). However, when pol η or pol $\kappa\Delta C$ was used, primer extension resulted in fully extended products. No blockage was detected at the dI adduct site. When the amounts of pols were increased, products representing more than 32-mer bases long were produced on the unmodified and dI-modified templates. Blunt-end addition to the fully extended product (33–34-mers) was observed, as reported earlier for *Escherichia coli* and mammalian DNA pols.^{26,27}

Miscoding frequencies and specificities of the dI adduct

Translesion synthesis catalyzed by pol α , pol η , or pol $\kappa\Delta C$ was conducted in the presence of all four dNTPs. The fully extended products (approximately 28–34-mers) past the unmodified or modified adducts were recovered, digested by EcoRI, and subjected to two-phased PAGE for quantitative analysis of base substitutions and deletions as described in Materials and Methods (Fig. 3). A standard mixture of six Alexa Fluor 546 dye (Alexa546)-labeled oligodeoxynucleotides containing dC, dA, dG, or dT opposite the lesion or one- and two-base deletions can be resolved by this method (Fig. 5). The percentage of 2'-deoxynucleoside monophosphate incorporation was normalized to the amount of the starting primer. When an unmodified dA template was used, expected incorporation of dTMP, the correct base, was observed opposite dA (Fig. 5). As indicated by the arrowhead in Fig. 5b, small amounts of unknown products were detected. When pol α was used with a template containing dI, dCMP (83.3% of the starting primers) was exclusively incorporated opposite the lesion. Similarly, pol η and pol $\kappa\Delta C$ promoted preferential incorporation of dCMP (55.0% and 74.7%, respectively) opposite the lesion. No deletions were detected. Surprisingly, no incorporation of dTMP, the correct base, was detected opposite the dI adduct with all pols, that is, pol α , pol η , and pol $\kappa\Delta C$.

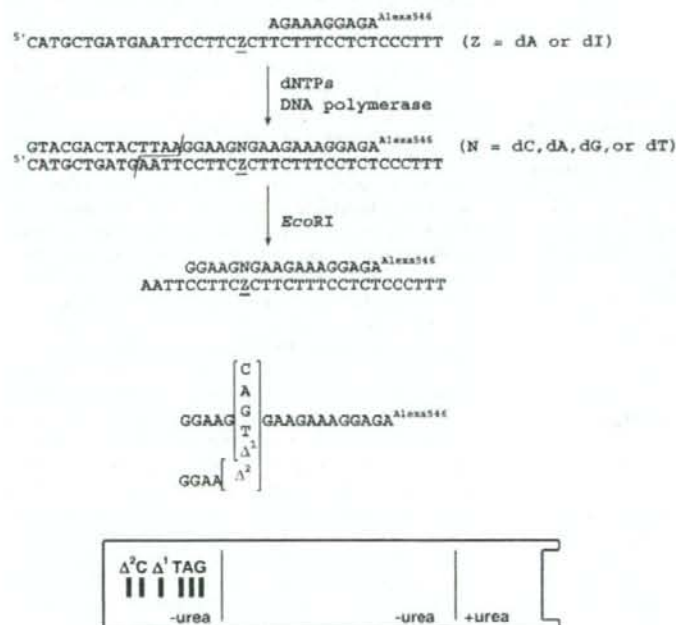


Fig. 3. Diagram of the fluorescent two-phased PAGE to determine miscoding specificity of DNA adducts. Unmodified and dI-modified 38-mer templates are annealed to either an Alexa546-labeled 10-mer primer or an Alexa546-labeled 12-mer primer. Primer extension reactions catalyzed by DNA pol α , pol η , or pol $\kappa\Delta C$ were conducted in the presence of four dNTPs. Fully extended products formed during DNA synthesis were recovered from the polyacrylamide gel (30 × 40 × 0.05 cm), annealed with a complementary 38-mer, cleaved with EcoRI, and subjected to a two-phased PAGE (20 × 65 × 0.05 cm), as described in Materials and Methods. To determine miscoding specificity, mobilities of the reaction products were compared with those of 18-mer standards containing dC, dA, dG, or dT opposite the lesion and one-base (Δ^1) or two-base (Δ^2) deletions.

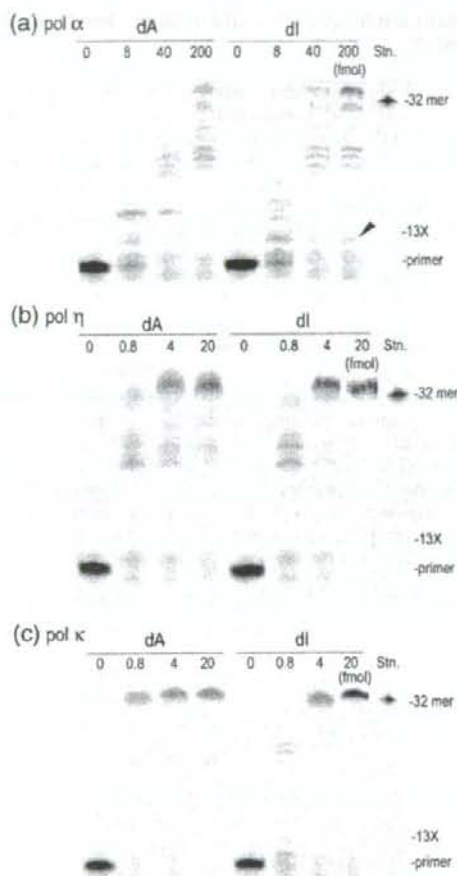


Fig. 4. Primer extension reactions catalyzed by pol α , pol η , or pol $\kappa\Delta C$ on dl-modified DNA template. Using unmodified or dl-modified 38-mer templates primed with an Alexa546-labeled 10-mer, we performed primer extension reactions at 25 °C for 30 min in a buffer containing four dNTPs (100 μ M each) and varying amounts of (a) pol α (0, 8, 40, and 200 fmol), (b) pol η , or (c) pol $\kappa\Delta C$ (0, 0.8, 4, and 20 fmol), as described in Materials and Methods. The whole amount of the reaction mixture was subjected to 20% denaturing PAGE (30 \times 40 \times 0.05 cm). An Alexa546-labeled 32-mer (5'AGAGGAAAGTAGCGAAGGAATTCATCAGCATG) was used as a marker of fully extended product. 13X represents the adducted position.

Kinetic studies on dl-modified templates

Steady-state kinetic studies were performed using pol α , pol η , and pol $\kappa\Delta C$ to determine the frequency of dNTP incorporation (F_{ins}) opposite the dl lesion and chain extension (F_{ext}) from the primer terminus using the same sequence context that was used for the two-phased PAGE assay (Table 1). With pol α , the F_{ins} value for deoxythymidine triphosphate (dTTP) (1.21×10^{-2}), the correct base, opposite the dl was 59

times lower than that for 2'-deoxycytidine triphosphate (dCTP) (0.718). The relative bypass frequency ($F_{ins} \times F_{ext}$) past the dC:dl pair was approximately 2100 times higher than that for the dT:dl pair. F_{ins} and F_{ext} values for dA:dI and dG:dI were not detectable. When pol η was used, the F_{ins} value for dCTP (0.551), the wrong base, opposite the dl was 27 times higher than that for dTTP (2.07×10^{-2}) and was 17 and 75 times higher than that for 2'-deoxyadenosine triphosphate and 2'-deoxyguanosine triphosphate (dGTP), respectively. The F_{ext} value for the dC:dl pair was also higher than that for other 2'-deoxynucleoside monophosphates paired with dl. As a result, the $F_{ins} \times F_{ext}$ value past dC:dl was at least 3 orders of magnitude higher than that past other pairs. Similarly, with pol κ , $F_{ins} \times F_{ext}$ past dC:dl was much higher than that for other base pairs. F_{ins} and F_{ext} values for dTTP were 119 and 55 times lower than that for dCTP, respectively. Thus, all pols, that is, pol α , pol η , and pol $\kappa\Delta C$, exclusively promote misincorporation of dCMP opposite the dl lesion during translesion synthesis, since $F_{ins} \times F_{ext}$ values of other dNTPs were considerably lower than that for dCTP, the wrong base.

Discussion

Primer extension reactions catalyzed by DNA pols are a powerful method to explore translesion synthesis past DNA adducts and their accompanying kinetic parameters of nucleotide insertion and extension. A 32 P-labeled oligodeoxynucleotide at the 5'-terminus is widely employed in such analyses; however, the handling of hazardous radioisotopes is intricate for use and waste disposal. Indeed, use of radioisotopes is restricted in many countries including Japan. As an alternative to 32 P, we used fluorescent dyes, Alexa546 and Cyanin 3 (Cy3), to label the 5'-terminus of the oligodeoxynucleotide used as primers and standard markers. The detection limits of Alexa546- and Cy3-labeled primers were approximately 120 and 240 times lower than that of the 32 P-labeled primer, respectively. However, when Alexa546-labeled primers (500 fmol) were annealed with DNA template (750 fmol) and the assays of primer extension and kinetic studies were carried out in this work, the resultant data were quantitative and reproducible (Figs. 6 and 7). Alexa546 exhibits a more sensitive and photostable fluorescence than Cy3. Moreover, even under repeated thawing and melting, an Alexa546-labeled oligomer stored at -20 °C was not degraded for at least 6 months. Using this method, we determined the miscoding frequency and specificity of 8-OxodG, which is known to generate predominantly 2'-deoxyadenosine monophosphate misincorporation at the lesion site. The results obtained from Alexa546 labeling were consistent with that from 32 P labeling (data not shown). Thus, Alexa546 was applicable to two-phased PAGE. Therefore, we have used this fluorescent method to explore translesion synthesis past dl adducts and its miscoding specificity and frequency using two-phased PAGE.

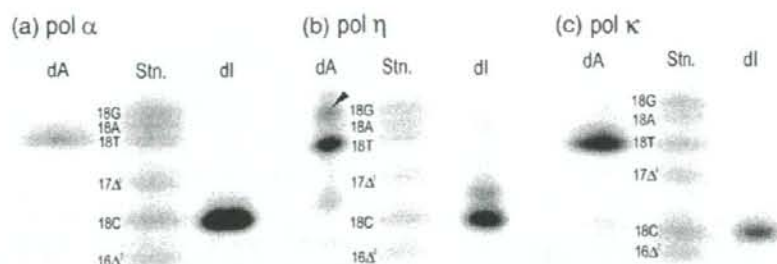


Fig. 5. Miscoding specificities of the dI lesion in reactions catalyzed by pol α , pol η , or pol $\kappa\Delta C$. Using unmodified and dI-modified 38-mer templates primed with an Alexa546-labeled 12-mer, we conducted primer extension reactions at 25 °C for 30 min in a buffer containing four dNTPs (100 μ M each) and either pol α (200 fmol for unmodified and dI-modified templates), pol $\kappa\Delta C$, or pol η (20 fmol for unmodified and dI-modified templates), as described in Materials and Methods. The extended reaction products (>26 bases long) produced on the unmodified and dI-modified templates were extracted following PAGE. The recovered oligodeoxynucleotides were annealed to an unmodified 38-mer and cleaved with EcoRI restriction enzyme, as described in Materials and Methods. The entire product from the unmodified and dI-modified templates was subjected to two-phased PAGE (20 \times 65 \times 0.05 cm). Mobilities of reaction products were compared with those of 18-mer standards (Fig. 3) containing dC, dA, dG, or dT opposite the lesion and one-base (Δ^1) or two-base (Δ^2) deletions.

The mutation spectrum induced by ^1NO has been investigated in a variety of experimental systems. ^1NO gas showed mutagenicity in TK6 cells¹⁰ and caused predominantly A:T \rightarrow G:C transitions in plasmids replicated in cultured human and *E. coli* cells^{28,29} and C \rightarrow T transitions in a bacterial system.⁹ Moreover, ^1NO -releasing compounds exclusively resulted in G:C \rightarrow A:T transitions in pSP189 plasmids propagated in human cells.³⁰ Using similar ^1NO -releasing compounds, ONOO $^-$ caused G:C \rightarrow T:A and G:C \rightarrow C:G transversions with the same experimental system.^{31,32} Thus, based on the information obtained from these previous reports, the mutation spectrum

by ^1NO has not been extensively determined yet.³³ In our previous studies, the miscoding frequencies and specificities of dX, 8-NO $_2$ -dG, and 8-OxodG lesions were quantitatively determined by two-phased PAGE. As a result, 8-NO $_2$ -dG³⁴ and 8-OxodG^{17,35} are miscoding lesions generating primarily G \rightarrow T transversions (~20% and ~38%, respectively), while the miscoding spectrum of the dX adduct³⁶ exclusively shows G \rightarrow A transitions (~50%), which differs from that of 8-NO $_2$ -dG and 8-OxodG. This indicates that each DNA adduct has a unique miscoding specificity and frequency. The mutation spectrum by ^1NO can be hardly determined due to the presence of diverse

Table 1. Kinetic parameters for nucleotide insertion and chain extension reactions catalyzed by human DNA pol α , pol η , and pol $\kappa\Delta C$.

	N:Z	Insertion dNTP			Extension dGTP			$F_{\text{ins}} \times F_{\text{ext}}$
		↓GAAGAAAGGAGA ^{Alexa546}			↓NGAAGAAAGGAGA ^{Alexa546}			
		5'CCTTCZCTTCITTCCTCCCTTT			5'CCTTCZCTTCITTCCTCCCTTT			
K_m (μ M) ^a	V_{max} (% min $^{-1}$) ^a	F_{ins}	K_m (μ M) ^a	V_{max} (% min $^{-1}$) ^a	F_{ext}			
Pol α	T:A	0.56 \pm 0.03	0.53 \pm 0.02	1.0	0.41 \pm 0.14	0.31 \pm 0.03	1.0	1.0
	C:Z	0.73 \pm 0.26	0.47 \pm 0.03	0.718	0.48 \pm 0.09	0.25 \pm 0.01	0.679	0.487
	A:Z	N.D.	N.D.	N.D.	N.D.	N.D.	N.D.	N.D.
	G:Z	N.D.	N.D.	N.D.	N.D.	N.D.	N.D.	N.D.
Pol η	T:Z	9.74 \pm 1.60	0.11 \pm 0.07	1.21 $\times 10^{-2}$	7.09 \pm 1.50	10.1 \pm 0.65	1.92 $\times 10^{-2}$	2.32 $\times 10^{-4}$
	T:A	0.65 \pm 0.17	5.37 \pm 0.26	21.0	0.69 \pm 0.13	7.49 \pm 0.11	1.0	1.0
	C:Z	1.74 \pm 0.58	7.79 \pm 0.48	0.551	0.96 \pm 0.18	8.44 \pm 0.25	0.809	0.446
	A:Z	4.87 \pm 1.22	1.28 \pm 0.03	3.18 $\times 10^{-2}$	6.63 \pm 0.76	2.66 \pm 0.08	3.66 $\times 10^{-2}$	1.16 $\times 10^{-3}$
Pol $\kappa\Delta C$	G:Z	16.1 \pm 1.03	1.00 \pm 0.01	7.30 $\times 10^{-3}$	11.6 \pm 4.23	1.14 \pm 0.11	9.40 $\times 10^{-3}$	6.86 $\times 10^{-5}$
	T:Z	7.00 \pm 1.97	1.19 \pm 0.03	2.07 $\times 10^{-2}$	6.76 \pm 0.41	4.99 \pm 0.02	6.72 $\times 10^{-2}$	1.39 $\times 10^{-3}$
	T:A	1.43 \pm 0.38	11.1 \pm 0.47	1.0	0.55 \pm 0.07	13.9 \pm 0.54	1.0	1.0
	C:Z	1.36 \pm 0.40	10.3 \pm 0.44	0.987	0.79 \pm 0.76	13.1 \pm 0.12	0.651	0.642
	A:Z	15.5 \pm 4.30	1.10 \pm 0.05	9.23 $\times 10^{-3}$	10.7 \pm 2.43	2.17 \pm 0.07	8.13 $\times 10^{-3}$	7.50 $\times 10^{-5}$
	G:Z	84.0 \pm 15.4	0.76 \pm 0.30	1.12 $\times 10^{-3}$	12.8 \pm 2.25	0.51 \pm 0.05	1.57 $\times 10^{-3}$	1.75 $\times 10^{-6}$
	T:Z	23.5 \pm 6.93	1.50 \pm 0.11	8.26 $\times 10^{-3}$	5.28 \pm 0.37	1.59 \pm 0.03	1.18 $\times 10^{-2}$	9.74 $\times 10^{-5}$

Kinetics of nucleotide insertion and chain extension reactions were determined as described in Materials and Methods. Frequencies of nucleotide insertion (F_{ins}) and chain extension (F_{ext}) were estimated by the following equation: $F = (V_{\text{max}}/K_m)_{\text{correct pair}} / (V_{\text{max}}/K_m)_{\text{correct pair} = \text{dT:dA}}$. Z = dA or dI lesion.

N.D., not detectable.

^a Data are expressed as mean \pm SD obtained from three independent experiments.

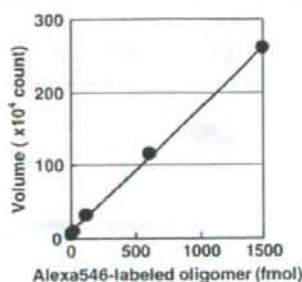


Fig. 6. Calibration curve using fluorescent oligomers labeled by Alexa546. Varying amounts of Alexa546-labeled oligomer were subjected to 20% denaturing PAGE. The volume of bands was quantitatively measured by using Molecular Imager FX Pro and Quantity One software (Bio-Rad) to find a linear range in the fluorescent analysis.

DNA adducts caused by $\cdot\text{NO}$ -involved species (Fig. 1) and its miscoding variety.^{17,34,35} Therefore, the quantitative miscoding properties of each $\cdot\text{NO}$ -derived DNA adduct must be required to explore its roles in the inflammation-driven carcinogenesis.

The miscoding specificity of dI was determined by using an *in vitro* experimental system that can quantify base substitutions and deletions formed during replication in the presence of four dNTPs. Pol α , pol η , and pol $\kappa\Delta\text{C}$ incorporated dCMP (83.3%, 55.0%, and 74.7%, respectively) preferentially opposite the dI lesion rather than dTMP, the correct base (Fig. 5). Kamiya *et al.* reported earlier that mouse pol α inserted dCMP and dTMP, the correct base, opposite the dI lesion.¹⁶ In contrast, human pol α promoted direct incorporation of dCMP only (Fig. 5). These indicate that the pols promote miscoding by incorporating dCMP opposite the dI lesion during DNA synthesis. Thus, dI is a highly miscoding lesion, generating A \rightarrow G transitions in human cells. Steady-state kinetic studies supported these results. When pol α , pol η , and pol $\kappa\Delta\text{C}$ were used, $F_{\text{ins}} \times F_{\text{ext}}$ values for dC:dI pairs were 2100, 320, and 6600 times higher than those for dT:dI pairs, respectively (Table 1). Therefore, the kinetic results were consistent with that observed using two-phased PAGE analysis. Taken together, both analyses showed that human

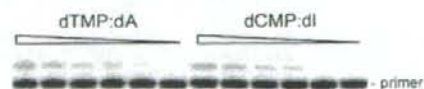


Fig. 7. Typical image of PAGE for kinetic studies performed by Alexa546 labeling. Using unmodified or dI-modified 38-mer templates (750 fmol) primed with an Alexa546-labeled 12-mer (500 fmol), we conducted primer extension reactions at 25 $^{\circ}\text{C}$ for 2 min in a buffer containing pol $\kappa\Delta\text{C}$ (1 fmol) and either dTTP (0.25–25 μM for unmodified templates) or dCTP (0.25–25 μM for dI-modified templates), as described in Materials and Methods. The whole amount of the reaction mixture was subjected to 20% denaturing PAGE (30 \times 40 \times 0.05 cm).

DNA pols miscode at dI lesions by exclusively incorporating dCMP. The miscoding specificity was consistent with that observed in *E. coli*,⁹ mammalian cells,^{10,37} and mice exposed to $\cdot\text{NO}$.¹⁵

To compare the relative bypass frequency of dI, dX, and 8-NO₂-dG by pol α , pol η , and pol $\kappa\Delta\text{C}$, these adducts were embedded in a similar sequence context^{34,36} (Table 2). With pol α , the $F_{\text{ins}} \times F_{\text{ext}}$ ratio for the dC:dI/dT:dI pairs was 2100. This number was remarkably higher than that for the dT:dX/dC:dX (ratio=1.5) or dA:8-NO₂-dG/dC:8-NO₂-dG (ratio=0.01) pairs. Similar results were observed with pol η and pol $\kappa\Delta\text{C}$. The ratios of $F_{\text{ins}} \times F_{\text{ext}}$ past dI were 2 orders of magnitude higher than those of dX and 8-NO₂-dG. Thus, dI adducts promote a higher miscoding potential (A \rightarrow G transitions) than those of dX or 8-NO₂-dG. However, the highly mutagenic dI lesions did not show serious mutation frequency^{9,10} even though they were predominantly paired with the wrong base, dCMP. Endonuclease V (endo V) has shown to be a dI-specific endonuclease.^{38–40} Methylpurine glycosylase also recognizes this lesion.^{41–43} For instance, *E. coli* cells lacking the endo V (*hfl*) gene were shown to exhibit elevated mutation frequencies when exposed to nitrous acid. The increased mutations were predominantly A:T \rightarrow G:C mutations, followed by lesser G:C \rightarrow A:T mutations.^{44,45} This indicates that endo V is primarily involved in the repair of dI lesions.^{44–48}

The structure of double-stranded oligodeoxynucleotide containing the dI:dC pair was determined by thermodynamic and NMR studies.^{49,50} dI can most stably pair with dC among four dNs, and its geometric structure is similar in form with the Watson-Crick structure (Fig. 8). dI has a carbonyl group at position C6 and a positive charge at position N1 after dA suffers from nitrosative deamination by $\cdot\text{NO}$. Thus, since the structure of dI is similar to that of dG rather than dA, the dI adduct can predominantly pair with dC, the wrong base.

In conclusion, nonradioactive kinetic studies and two-phased PAGE were performed to explore the

Table 2. $F_{\text{ins}} \times F_{\text{ext}}$ past DNA adducts by human DNA pol α , pol η , and pol $\kappa\Delta\text{C}$

	Z=	dI ^a	dX ^b	8-NO ₂ -dG ^c
Pol α	C:Z	0.487	4.50×10^{-3}	1.69×10^{-3}
	A:Z	N.D.	2.18×10^{-4}	1.31×10^{-5}
	G:Z	N.D.	1.11×10^{-5}	2.63×10^{-6}
Pol η	T:Z	2.32×10^{-4}	6.68×10^{-3}	5.87×10^{-6}
	C:Z	0.446	5.24×10^{-2}	6.94×10^{-3}
	A:Z	1.16×10^{-3}	1.71×10^{-3}	5.09×10^{-3}
Pol $\kappa\Delta\text{C}$	G:Z	6.86×10^{-5}	2.94×10^{-4}	4.63×10^{-4}
	T:Z	1.39×10^{-3}	0.259	4.06×10^{-4}
	C:Z	0.642	8.39×10^{-3}	6.37×10^{-5}
	A:Z	7.50×10^{-5}	2.43×10^{-6}	2.88×10^{-5}
	G:Z	1.75×10^{-6}	2.48×10^{-6}	2.62×10^{-6}
	T:Z	9.74×10^{-3}	5.12×10^{-2}	6.62×10^{-7}

Values in boldface show a primarily misincorporated base opposite the DNA adduct.

N.D., not detectable.

^a Data were taken from Table 1.

^b Data were taken from Ref. 36.

^c Data were taken from Ref. 34.

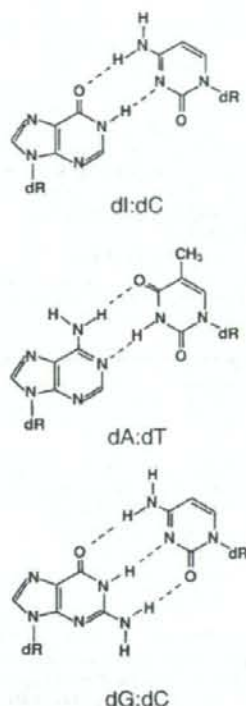


Fig. 8. Possible base pairing of the dI adduct with dC.

miscoding specificities and frequencies of the dI lesion catalyzed by Y-family human DNA pols. The dI adduct represents a highly miscoding lesion capable of generating A→G transitions, indicating that this NO-induced lesion plays an important role in initiating inflammation-driven carcinogenesis.

Materials and Methods

General

Ultrapure dNTPs were from GE Healthcare. EcoRI restriction endonuclease (100 U/ μ L) was purchased from New England BioLabs. Blue Dextran (D5751) was obtained from Sigma. Human pol α was obtained from CHIMERx (Milwaukee, WI). Human pol η was purified as previously described.¹⁹ Human pol κ (pol $\kappa\Delta C$) was overexpressed in *E. coli* and purified as a C-terminally truncated form. The protein has 10 \times His tag at the N-terminal position and contains 559 amino acids from the N-terminus (N. Niimi and T. Nohmi *et al.*, unpublished results).

Preparation of oligodeoxynucleotides

All oligodeoxynucleotides, Alexa546 (Molecular Probes)-labeled primers, standard markers, and dI-modified template were obtained from Japan Bio Service Co. (Saitama,

Japan). Alexa546 was conjugated at the 5'-terminus of primers and standard markers. A single dI was located at the 20th position from the 5'-termini in the modified 38-mer template (5'-CATGCTGATGAATTCCTTCZCTTCCTTCCTCCCTTT, where Z is dI). The oligomers were purified by using 20% denaturing PAGE before use.

Primer extension reactions

Primer extension reactions catalyzed by pol α , pol η , or pol $\kappa\Delta C$ were conducted at 25 $^{\circ}$ C for 30 min in a buffer (10 μ L) containing all four dNTPs (100 μ M each) using dI-modified and unmodified 38-mer templates (750 fmol) primed with an Alexa546-labeled 10-mer (500 fmol, 5'-AGAGGAAAGA) (Fig. 3). The reaction buffer for pol α contains 40 mM Tris-HCl (pH 8.0), 5 mM MgCl₂, 60 mM KCl, 10 mM dithiothreitol, 250 μ g/mL bovine serum albumin, and 2.5% glycerol. The reaction buffer for pol η and pol $\kappa\Delta C$ contains 40 mM Tris-HCl (pH 8.0), 1 mM MgCl₂, 10 mM dithiothreitol, 250 μ g/mL bovine serum albumin, 60 mM KCl, and 2.5% glycerol. Reaction was stopped by addition of 2 μ L formamide dye containing Blue Dextran (100 mg/mL) and ethylenediaminetetraacetic acid (50 mM) and incubation at 95 $^{\circ}$ C for 3 min. The whole amount of the reaction sample was subjected to 20% denaturing PAGE (30 \times 40 \times 0.05 cm). The positions of bands and homogeneities of oligodeoxynucleotides following PAGE were determined by using Molecular Imager FX Pro and Quantity One software (Bio-Rad). The linear range to quantitatively detect fluorescence-labeled oligomers was from 5 to 1500 fmol (Fig. 6).

Quantitation of miscoding specificity

Using dI-modified and unmodified 38-mer oligodeoxynucleotide (750 fmol) primed with an Alexa546-labeled 12-mer (500 fmol, 5'-AGAGGAAAGA), we conducted primer extension reactions catalyzed by pol α (200 fmol), pol η (20 fmol), or pol $\kappa\Delta C$ (20 fmol) at 25 $^{\circ}$ C for 30 min in a buffer (10 μ L) containing all four dNTPs (100 μ M each) and subjected them to 20% denaturing PAGE (30 \times 40 \times 0.05 cm). Extended reaction products (>26 bases long) were extracted from the gel. The recovered oligodeoxynucleotides were annealed with an unmodified 38-mer, cleaved with EcoRI, and subjected to two-phased PAGE (20 \times 65 \times 0.05 cm) containing 7 M urea in the upper phase and no urea in the middle and bottom phases (each phase contains 18%, 20%, and 24% polyacrylamide, respectively). The phase width is approximately 10, 37, and 18 cm from the upper phase. To quantify base substitutions and deletions, we compared the mobility of the reaction products with those of Alexa546-labeled 18-mer standards containing dC, dA, dG, or dT opposite the lesion and one-base (Δ^1) or two-base (Δ^2) deletions^{17,18} (Fig. 3).

Steady-state kinetic studies of nucleotide insertion and extension

Kinetic parameters associated with nucleotide insertion opposite the dI lesion and chain extension from the 3' primer terminus were determined at 25 $^{\circ}$ C, using varying amounts of single dNTPs. For insertion kinetics, reaction mixtures containing dNTP (0–250 μ M) and either pol α (20–200 fmol), pol η (2–20 fmol), or pol $\kappa\Delta C$ (1–20 fmol) were incubated at 25 $^{\circ}$ C for 2 min in 10 μ L of Tris-HCl buffer (pH 8.0) using a 38-mer template (750 fmol) primed with an Alexa546-labeled 12-mer (500 fmol; 5'-AGAG-

GAAAGAAG). Reaction mixtures containing a 38-mer template (750 fmol) primed with an Alexa546-labeled 13-mer (500 fmol; 5'AGAGGAAAGAAGN, where N is C, A, G, or T), with varying amounts of dGTP (0–250 μ M) and either pol α (20–200 fmol), pol η (1–20 fmol), or pol κ Δ C (1–20 fmol), were used to measure chain extension. The reaction samples were subjected to 20% denaturing PAGE (30 \times 40 \times 0.05 cm). The Michaelis constants (K_m) and maximum rates of reaction (V_{max}) were obtained from Hanes–Woolf plots. Frequencies of dNTP insertion (F_{ins}) and chain extension (F_{ext}) were determined relative to the dT:dA base pair according to the following equation: $F = (V_{max}/K_m)_{[wrong\ pair]} / (V_{max}/K_m)_{[correct\ pair = dT:dA]}$ ^{24,25}

Acknowledgements

This research was supported in part by Grants-in-aid for Scientific Research 19710059 from the Ministry of Education, Culture, Sports, Science and Technology (to M.Y.). This work was also partially supported by Health, Welfare, and Labor Science Research Grants (H18-food-general-009) and a Grant-in-aid (KHB1007) from the Japan Health Science Foundation (to M.H.).

References

- Ohshima, H. & Bartsch, H. (1994). Chronic infections and inflammatory processes as cancer risk factors: possible role of nitric oxide in carcinogenesis. *Mutat. Res.* **305**, 253–264.
- Cassell, G. H. (1998). Infectious causes of chronic inflammatory diseases and cancer. *Emerg. Infect. Dis.* **4**, 475–487.
- Ohshima, H., Tatemichi, M. & Sawa, T. (2003). Chemical basis of inflammation-induced carcinogenesis. *Arch. Biochem. Biophys.* **417**, 3–11.
- Burney, S., Caulfield, J. L., Niles, J. C., Wishnok, J. S. & Tannenbaum, S. R. (1999). The chemistry of DNA damage from nitric oxide and peroxynitrite. *Mutat. Res.* **424**, 37–49.
- deRojas-Walker, T., Tamir, S., Ji, H., Wishnok, J. S. & Tannenbaum, S. R. (1995). Nitric oxide induces oxidative damage in addition to deamination in macrophage DNA. *Chem. Res. Toxicol.* **8**, 473–477.
- Yermilov, V., Rubio, J., Becchi, M., Friesen, M. D., Pignatelli, B. & Ohshima, H. (1995). Formation of 8-nitroguanine by the reaction of guanine with peroxynitrite *in vitro*. *Carcinogenesis*, **16**, 2045–2050.
- Yermilov, V., Rubio, J. & Ohshima, H. (1995). Formation of 8-nitroguanine in DNA treated with peroxynitrite *in vitro* and its rapid removal from DNA by depurination. *FEBS Lett.* **376**, 207–210.
- Lewis, R. S., Tannenbaum, S. R. & Deen, W. M. (1995). Kinetics of N-nitrosation in oxygenated nitric oxide solutions at physiological pH: role of nitrous anhydride and effects of phosphate and chloride. *J. Am. Chem. Soc.* **117**, 3933–3939.
- Wink, D. A., Kasprzak, K. S., Maragos, C. M., Elespuru, R. K., Misra, M., Dunams, T. M. *et al.* (1991). DNA deaminating ability and genotoxicity of nitric oxide and its progenitors. *Science*, **254**, 1001–1003.
- Nguyen, T., Brunson, D., Crespi, C. L., Penun, B. W., Wishnok, J. S. & Tannenbaum, S. R. (1992). DNA damage and mutation in human cells exposed to nitric oxide *in vitro*. *Proc. Natl. Acad. Sci. USA*, **89**, 3030–3034.
- Caulfield, J. L., Wishnok, J. S. & Tannenbaum, S. R. (1998). Nitric oxide-induced deamination of cytosine and guanine in deoxynucleosides and oligonucleotides. *J. Biol. Chem.* **273**, 12689–12695.
- Dong, M., Wang, C., Deen, W. M. & Dedon, P. C. (2003). Absence of 2'-deoxyoxanosine and presence of abasic sites in DNA exposed to nitric oxide at controlled physiological concentrations. *Chem. Res. Toxicol.* **16**, 1044–1055.
- Pang, B., Zhou, X., Yu, H., Dong, M., Taghizadeh, K., Wishnok, J. S. *et al.* (2007). Lipid peroxidation dominates the chemistry of DNA adduct formation in a mouse model of inflammation. *Carcinogenesis*, **28**, 1807–1813.
- Dong, M. & Dedon, P. C. (2006). Relatively small increases in the steady-state levels of nucleobase deamination products in DNA from human TK6 cells exposed to toxic levels of nitric oxide. *Chem. Res. Toxicol.* **19**, 50–57.
- Gal, A. & Wogan, G. N. (1996). Mutagenesis associated with nitric oxide production in transgenic SJL mice. *Proc. Natl. Acad. Sci. USA*, **93**, 15102–15107.
- Kamiya, H., Sakaguchi, T., Murata, N., Fujimuro, M., Miura, H., Ishikawa, H. *et al.* (1992). *In vitro* replication study of modified bases in ras sequences. *Chem. Pharm. Bull.* **40**, 2792–2795.
- Masutani, C., Araki, M., Yamada, A., Kusumoto, R., Nogimori, T., Maekawa, T. *et al.* (1999). Xeroderma pigmentosum variant (XP-V) correcting protein from HeLa cells has a thymine dimer bypass DNA polymerase activity. *EMBO J.* **18**, 3491–3501.
- Ogi, T., Kato, T., Jr, Kato, T. & Ohmori, H. (1999). Mutation enhancement by DINB1, a mammalian homologue of the *Escherichia coli* mutagenesis protein dinB. *Genes Cells*, **4**, 607–618.
- Gerlach, V. L., Aravind, L., Gotway, G., Schultz, R. A., Koonin, E. V. & Friedberg, E. C. (1999). Human and mouse homologs of *Escherichia coli* DinB (DNA polymerase IV), members of the UmuC/DinB superfamily. *Proc. Natl. Acad. Sci. USA*, **96**, 11922–11927.
- Goodman, M. F. & Tippen, B. (2000). The expanding polymerase universe. *Nat. Rev. Mol. Cell Biol.* **1**, 101–109.
- Kunkel, T. A., Pavlov, Y. L. & Bebenek, K. (2003). Functions of human DNA polymerases η , κ and ι suggested by their properties, including fidelity with undamaged DNA templates. *DNA Repair*, **3**, 135–149.
- Shibutani, S. (1993). Quantitation of base substitutions and deletions induced by chemical mutagens during DNA synthesis *in vitro*. *Chem. Res. Toxicol.* **6**, 625–629.
- Shibutani, S., Suzuki, N., Matsumoto, Y. & Grollman, A. P. (1996). Miscoding properties of 3,N⁴-etheno-2'-deoxycytidine in reactions catalyzed by mammalian DNA polymerases. *Biochemistry*, **35**, 14992–14998.
- Mendelman, L. V., Boosalis, M. S., Petruska, J. & Goodman, M. F. (1989). Nearest neighbor influences on DNA polymerase insertion fidelity. *J. Biol. Chem.* **264**, 14415–14423.
- Mendelman, L. V., Petruska, J. & Goodman, M. F. (1990). Base mispair extension kinetics. Comparison of DNA polymerase alpha and reverse transcriptase. *J. Biol. Chem.* **265**, 2338–2346.
- Clark, J. M., Joyce, C. M. & Beardsley, G. P. (1987). Novel blunt-end addition reactions catalyzed by DNA polymerase I of *Escherichia coli*. *J. Mol. Biol.* **198**, 123–127.

27. Terashima, I., Suzuki, N., Dasaradhi, L., Tan, C.-K., Downey, K. M. & Shibutani, S. (1998). Translesional synthesis on DNA templates containing an estrogen quinone derived adduct: N^2 -(2-hydroxyestron-6-yl)-2'-deoxyguanosine and N^6 -(2-hydroxyestron-6-yl)-2'-deoxyadenosine. *Biochemistry*, **37**, 13807-13815.
28. Routledge, M. N., Wink, D. A., Keefer, L. K. & Dipple, A. (1993). Mutations induced by saturated aqueous nitric oxide in the pSP189 *supF* gene in human Ad293 and *E. coli* MBM7070 cells. *Carcinogenesis*, **14**, 1251-1254.
29. Kelman, D. J., Christodolou, D., Wink, D. A., Keefer, L. K., Srinivasan, A. & Dipple, A. (1997). Relative mutagenicities of gaseous nitrogen oxides in the *supF* gene of pSP189. *Carcinogenesis*, **18**, 1045-1048.
30. Routledge, M. N., Wink, D. A., Keefer, L. K. & Dipple, A. (1994). DNA sequence changes induced by two nitric oxide donor drugs in the *supF* assay. *Chem. Res. Toxicol.* **7**, 628-632.
31. Juedes, M. J. & Wogan, G. N. (1996). Peroxynitrite-induced mutation spectra of pSP189 following replication in bacteria and in human cells. *Mutat. Res.* **349**, 51-61.
32. Kim, M. Y., Dong, M., Dedon, P. C. & Wogan, G. N. (2005). Effects of peroxynitrite dose and dose rate on DNA damage and mutation in the *supF* shuttle vector. *Chem. Res. Toxicol.* **18**, 76-86.
33. Routledge, M. N. (2000). Mutations induced by reactive nitrogen oxide species in the *supF* forward mutation assay. *Mutat. Res.* **450**, 95-105.
34. Suzuki, N., Yasui, M., Geacintov, N. E., Shafirovich, V. & Shibutani, S. (2005). Miscoding events during DNA synthesis past the nitration-damaged base 8-nitroguanine. *Biochemistry*, **44**, 9238-9245.
35. Shibutani, S., Takeshita, M. & Grollman, A. P. (1991). Insertion of specific bases during DNA synthesis past the oxidation-damaged base 8-oxodG. *Nature*, **349**, 431-434.
36. Yasui, M., Suzuki, N., Miller, H., Matsuda, T., Matsui, S. & Shibutani, S. (2004). Translesion synthesis past 2'-deoxyxanthosine, a nitric oxide-derived DNA adduct, by mammalian DNA polymerases. *J. Mol. Biol.* **344**, 665-674.
37. Kamiya, H., Miura, H., Kato, H., Nishimura, S. & Ohtsuka, E. (1992). Induction of mutation of a synthetic *c-Ha-ras* gene containing hypoxanthine. *Cancer Res.* **52**, 1836-1839.
38. Yao, M. & Kow, Y. W. (1996). Cleavage of insertion/deletion mismatches, flap and pseudo-Y DNA structures by deoxyinosine 3'-endonuclease from *Escherichia coli*. *J. Biol. Chem.* **271**, 30672-30676.
39. Yao, M., Hatahet, Z., Melamed, R. J. & Kow, Y. W. (1994). Purification and characterization of a novel deoxyinosine-specific enzyme, deoxyinosine 3' endonuclease, from *Escherichia coli*. *J. Biol. Chem.* **269**, 16260-16268.
40. Yao, M. & Kow, Y. W. (1995). Interaction of deoxyinosine 3'-endonuclease from *Escherichia coli* with DNA containing deoxyinosine. *J. Biol. Chem.* **270**, 28609-28616.
41. Saparbaev, M. & Laval, J. (1994). Excision of hypoxanthine from DNA containing dIMP residues by the *Escherichia coli*, yeast, rat, and human alkylpurine DNA glycosylases. *Proc. Natl. Acad. Sci. USA*, **91**, 5873-5877.
42. Fortini, P., Parlanti, E., Sidorkina, O. M., Laval, J. & Dogliotti, E. (1999). The type of DNA glycosylase determines the base excision repair pathway in mammalian cells. *J. Biol. Chem.* **274**, 15230-15236.
43. Miao, F., Bouziane, M. & O'Connor, T. R. (1998). Interaction of the recombinant human methylpurine-DNA glycosylase (MPG protein) with oligodeoxyribonucleotides containing either hypoxanthine or abasic sites. *Nucleic Acids Res.* **26**, 4034-4041.
44. Schouten, K. A. & Weiss, B. (1999). Endonuclease V protects *Escherichia coli* against specific mutations caused by nitrous acid. *Mutat. Res.* **435**, 245-254.
45. Weiss, B. (2006). Evidence for mutagenesis by nitric oxide during nitrate metabolism in *Escherichia coli*. *J. Bacteriol.* **188**, 829-833.
46. Guo, G. & Weiss, B. (1998). Endonuclease V (*nfi*) mutant of *Escherichia coli* K-12. *J. Bacteriol.* **180**, 46-51.
47. Dong, M., Vongchampa, V., Gingipalli, L., Cloutier, J. F., Kow, Y. W., O'Connor, T. & Dedon, P. C. (2006). Development of enzymatic probes of oxidative and nitrosative DNA damage caused by reactive nitrogen species. *Mutat. Res.* **594**, 120-134.
48. Weiss, B. (2001). Endonuclease V of *Escherichia coli* prevents mutations from nitrosative deamination during nitrate/nitrite respiration. *Mutat. Res.* **461**, 301-309.
49. Kawase, Y., Iwai, S., Inoue, H., Miura, K. & Ohtsuka, E. (1986). Studies on nucleic acid interactions. I. Stabilities of mini-duplexes (dG2A4XA4G2-dC2T4YT4C2) and self-complementary d(GGGAAXYTCCC) containing deoxyinosine and other mismatched bases. *Nucleic Acids Res.* **14**, 7727-7736.
50. Uesugi, S., Oda, Y., Ikehara, M., Kawase, Y. & Ohtsuka, E. (1987). Identification of IA mismatch base-pairing structure in DNA. *J. Biol. Chem.* **262**, 6965-6968.

Repair of I-SceI Induced DSB at a specific site of chromosome in human cells: influence of low-dose, low-dose-rate gamma-rays

Fumio Yatagai · Masao Suzuki · Noriaki Ishioka · Hitoshi Ohmori · Masamitsu Honma

Received: 9 January 2008 / Accepted: 5 June 2008 / Published online: 21 June 2008
© Springer-Verlag 2008

Abstract We investigated the influence of low-dose, low-dose-rate gamma-ray irradiation on DNA double strand break (DSB) repair in human lymphoblastoid TK6 cells. A single DSB was introduced at intron 4 of the *TK+* allele (chromosome 17) by transfection with the I-SceI expression vector pCBASce. We assessed for DSB repair due to non-homologous end-joining (NHEJ) by determining the generation of TK-deficient mutants in the TK6 derivative TSCE5 (*TK +/-*) carrying an I-SceI recognition site. We similarly estimated DSB repair via homologous recombination (HR) at the same site in the derived compound heterozygote (*TK -/-*) cell line TSCER2 that carries an additional point mutation in exon 5. The NHEJ repair of DSB was barely influenced by pre-irradiation of the cells with 30 mGy γ -rays at 1.2 mGy h^{-1} . DSB repair by HR, in contrast, was enhanced by $\sim 50\%$ after pre-irradiation of the cells under these conditions. Furthermore, when I-SceI digestion was followed by irradiation at a dose of 8.5 mGy,

delivered at a dose rate of only 0.125 mGy h^{-1} , HR repair efficiency was enhanced by $\sim 80\%$. This experimental approach can be applied to characterize DSB repair in the low-dose region of ionizing radiation.

Introduction

Health risks from low doses of ionizing radiation (IR) are of concern and it is important to estimate such risks for persons occupationally exposed to IR, such as airline crews, astronauts, and some workers in medical and industrial fields, including those in nuclear plants. Genetic analyses for induction of mutations, chromosome aberrations, micronuclei etc., are frequently used to estimate radiation risk. A new sensitive methodology developed in Honma's laboratory—analysis of loss of heterozygosity (LOH) at the *thymidine kinase (TK)* locus in human lymphoblastoid TK6 cells [1, 2]—can detect LOH events (interstitial deletions) in cells exposed to low doses of γ -rays delivered at a low dose rate, such as 30 mGy delivered at 1.2 mGy h^{-1} [3]. The LOH events are most likely a consequence of inaccurate repair of DNA double-strand breaks (DSBs), the most dangerous DNA lesion induced by IR. The high frequency of interstitial deletions observed after a low dose (30 mGy) exposure was unexpected because the estimated probability of generating two DSBs in the *TK* locus region is low under these conditions ($<2.25 \times 10^{-10}$) [3]. Thus, the radiation-induced DSBs seem unlikely to initiate the interstitial deletions. Rather, the deletions might result from IR interfering with correct repair of spontaneous DSBs or from the conversion of other damage, such as single-strand breaks.

When we tried to explore the influence of low-dose IR on DSB repair, we found it difficult to track specifically DSBs

F. Yatagai (✉) · H. Ohmori
Advanced Development and Support Center,
The Institute of Physical and Chemical Research (RIKEN),
Saitama 351-0198, Japan
e-mail: yatagai@postman.riken.go.jp

M. Suzuki
Heavy-ion Medical Science Center,
National Institute of Radiological Sciences,
Chiba-shi, Chiba, Japan

N. Ishioka
Japan Aerospace Exploration Agency,
Institute of Space and Astronautical Science,
Tsukuba-shi, Ibaraki, Japan

M. Honma
Division of Genetics and Mutagenesis,
National Institute of Health Sciences, Tokyo, Japan

amid the variety of DNA lesions that were induced. We therefore constructed a model system that could trace the fate of a single DSB [4, 5]. Our system can distinguish two major DSB repair pathways, non-homologous end-joining (NHEJ) and homologous recombination (HR) [6, 7]. NHEJ joins broken ends, which have little or no sequence homology in a non-conservative manner, and some information may be lost in the course of the repair process. HR, on the other hand, requires extensive tracts of sequence homology and is generally considered as error-free [8].

The human cell line TSCE5 is heterozygous (+/−) for the *TK* gene and the line TSCER2 is compound heterozygous (−/−); both carry an I-SceI endonuclease recognition site in intron 4 of one allele of the *TK* gene. DSBs can be generated at the I-SceI site by expression of the I-SceI vector [4]. When DSBs occur at the *TK* locus, NHEJ in TSCE5 cells produces TK-deficient mutants while HR between the *TK* alleles in TSCER2 cells produces TK-proficient revertants. This means that positive–negative drug selection for TK phenotypes permits distinction between NHEJ and HR repair.

The LOH analysis of TK mutants suggests that low-dose, low-dose-rate IR has important indirect effects. When the I-SceI model system is applied to estimating the influence of low-level IR on repair of a specifically introduced DSB, we can estimate the indirect effects of the exposure because the IR-damaged site can be ignored as a repair target. Here, we first examined whether such indirect effect can be detected by an experiment based upon the original concept of radioadaptation, a priming exposure to low-dose, low-dose-rate IR followed by the challenging treatment of I-SceI digestion. Second, a new type of experiment, the I-SceI treatment followed by low-dose, low-dose-rate IR exposure, was performed to investigate certain kinds of indirect effect, such as an influence of high radiation background exposure on DSB repair, because the continuous expression of I-SceI vector after the cell transfection mimics the above situation. These experiments provided the interesting finding that low level IR enhances the HR pathway.

Materials and methods

Cell line construction

Figure 1 outlines the structure of the repair substrates and the cell lines; the details of the strain construction were described previously [4]. Briefly, in lymphoblastoid TK6 cells heterozygous for the *TK* gene, the functional allele was first inactivated by gene targeting with vector pTK4 to replace exon 5 of the *TK* gene by a *neo* gene. To introduce the I-SceI recognition site, in a second step the targeting vector, pTK10, encompassing about 6 kb of the original *TK*

gene with exons 5, 6, and 7, and the I-SceI recognition site in intron 4, 75 bp upstream of exon 5, was used to revert the *TK* gene disrupted by pTK4. The new line was termed TSCE5. A spontaneous reversion in a TSCE5 cell (G to A in position 23 of exon 5), which we cloned, led to the compound heterozygote (*TK*−/−) cell line, TSCER2. In TSCE5, when a DSB at the I-SceI site is repaired by NHEJ involving a deletion in the adjacent exon, the cell can be isolated as a TK-deficient mutant. In TSCER2, when a DSB is repaired by HR between the *TK* alleles, a *TK*⁺ allele can be generated, resulting in a revertant phenotype.

Cell culture and IR exposure

Cell culture details were described in earlier work [1–3]. We tested the response of TSCE5 and TSCER2 cells cultured in RPMI1640 medium to low-dose, low-dose-rate γ -irradiation in a 5% CO₂ incubator both before (mode A, Fig. 2) and after (mode B, Fig. 2) I-SceI digestion. In mode A, the cells were exposed to ⁶⁰Co γ -rays at 1.2 mGy h^{−1} for 25 h (total exposure, 30 mGy) and reached a cell concentration of 8×10^5 ml^{−1} at the end of the irradiation/culture period. Then, 2 h after finishing the γ -irradiation, the cells were transfected with the I-SceI expression vector. The delay occurred because the radiation exposure facility was located far from the biological experimental area. In mode B, the cells were transfected with the vector first and 2 h later exposed to a much lower γ -ray dose and dose-rate (~28% of the mode A dose at ~10% of the mode A dose rate), namely 0.125 mGy h^{−1} for 68 h (total exposure, 8.5 mGy). In an independent determination performed with 8 cell culture flasks in duplicate experiments, cells were exposed for 96 h (total exposure, 12 mGy). At the end of irradiation/culture period in mode B, the cell concentration was adjusted to 8×10^5 ml^{−1}. Control cells were treated in the same manner except that they were not irradiated. The γ -irradiations were performed at the National Institute of Radiological Studies (NIRS), and the adjustment of dose-rate was done by changing the distance between the ⁶⁰Co source and the CO₂ incubator.

I-SceI expression

We introduced the I-SceI expression vector (pCBASce) by suspending 5×10^6 cells in 0.1 ml Nucleofector Solution V (amaxa AG, Cologne, Germany) with 50 μ g of uncut pCBASce vector, or without the vector as a control, following the manufacturer's recommendations [5]. Although we could not determine the efficiency of DSB generation under the present condition of transfection, the I-SceI expression vector was introduced into about 65% of the cells at 24 h after the transfection and the expression lasts for 3 days incubation [5].

Fig. 1 Strategy of DSB repair assays for I-SceI double strand breaks. The two constructed cell lines—the original TSCSE5 line containing the I-SceI recognition insert and its derived compound heterozygote TSCER2—are shown together with the selectable phenotypes generated by repair of double strand breaks (DSBs) through non-homologous end-joining (NHEJ) in TSCSE5 cells or homologous repair (HR) in TSCER2 cells (see text)

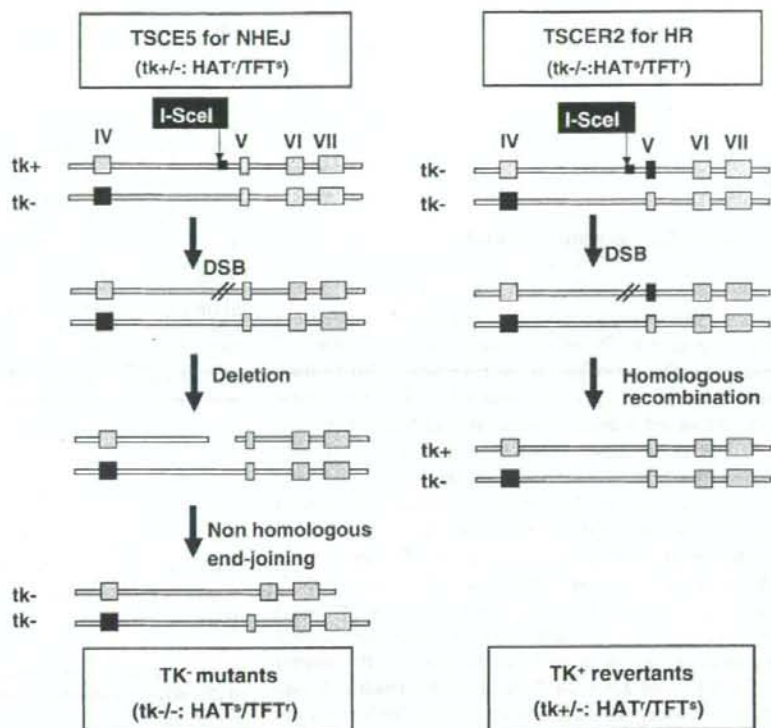
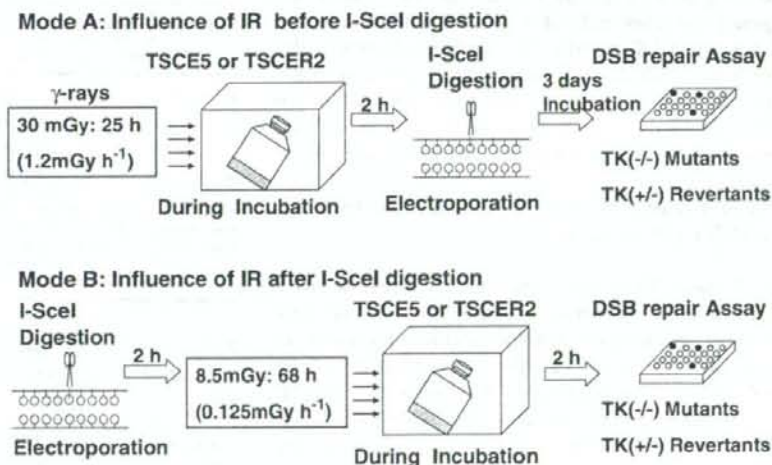


Fig. 2 Experimental scheme of radiation exposure and I-SceI expression. In mode A, cells were exposed to low-dose, low-dose-rate γ -irradiation and then transfected with the I-SceI vector by electroporation (see text). In mode B cells were transfected with the I-SceI vector and then exposed to γ -irradiation at a much lower dose and dose-rate (see text)



Determination of TK⁻ mutants and TK⁺ revertants

In mode A, immediately after transfection the cells were suspended in 50 ml of fresh RPMI1640 medium, incubated for 3 days, and then seeded into 96-microwell plates. In

mode B, the cell seeding was done at 2 h after the irradiation/incubation following the I-SceI digestion as described above. TSCSE5 cells were seeded at 100 cells per well and incubated in the presence of $2.0 \mu\text{g ml}^{-1}$ trifluorothymidine (TFT) for the detection of TK-deficient

mutants. TSCER2 cells were seeded at 2,000 cells per well in the presence of HAT (200 μ M hypoxanthine, 0.1 μ M aminopterin, 17.5 μ M thymidine) for the detection of TK-proficient revertants.

Results

TK mutant frequency after γ -irradiation

Table 1a shows frequencies of TK⁻ mutants in TSCE5 cells not expressing I-SceI without irradiation (control) and after exposure to 30 mGy γ -irradiation at 1.2 mGy h⁻¹ (mode A). The mean TK⁻ mutant frequency (MF) values were found to be 2.7×10^{-6} and 4.7×10^{-6} for control and γ -irradiated sample, respectively, and both the level of MFs and the increase caused by γ -irradiation were consistent with those of a previous investigation [3]. Table 2a shows TK⁻ mutant frequency in unirradiated control TSCE5 cells and cells that were exposed to 8.5 mGy γ -irradiation at 0.125 mGy h⁻¹ (mode B). The mean TK⁻ MF values for un- and γ -irradiated cells in the mode B experiment (3.0×10^{-6} and 2.1×10^{-6} , respectively) were very similar to values obtained after the 12 mGy exposure (at the same dose-rate as in mode B), namely 3.2×10^{-6} and 2.0×10^{-6} for un- and γ -irradiated sample, respectively. These results suggest that the lower doses (8.5 and 12 mGy) delivered at a lower dose rate (0.125 mGy h⁻¹) did not enhance the TK⁻ mutant frequency but rather reverted it. We did not determine the frequency of TK⁺ revertants for unirradiated control and γ -irradiated TSCER2 cells because we expected those frequencies to be too low for us to accurately estimate the effect of IR exposure. In fact, the spontaneous revertant frequency (RF) in TSCER2 is in the range of 10^{-8} [4, 5].

Effect of radiation exposure prior to I-SceI transfection on DSB repair (mode A)

In the mode A experiment, the low-dose, low-dose-rate γ -irradiation was performed prior to transfection with the I-SceI vector to estimate the influence of pre-IR exposure on repair of I-SceI introduced DSB. We calculated the relative TK⁻ mutant frequency $MF_{rel} = (MF(\gamma\text{-rays} + I\text{-SceI})/MF(I\text{-SceI}))$ for each experiment because the transfection efficiencies varied. The mean MF_{rel} in TSCE5 cells exposed to IR prior to transfection was 1.0 (Table 1a), indicating that irradiation had no effect on NHEJ repair of I-SceI-induced DSBs. The relative TK⁺ revertant frequency, RF_{rel} in TSCER2 cells was determined in an analogous manner. Exposure to irradiation prior to transfection consistently enhanced RF_{rel} , and the mean RF_{rel} was 1.5 (Table 1b), indicating that irradiation enhanced the

Table 1 Effect on DSB repair of exposure to 30 mGy IR at 1.2 mGy h⁻¹ prior to transfection with I-SceI expression vector (mode A)

Exp.	TK ⁻ Mutant Frequency, MF ($\times 10^{-6}$)				Effect of IR (MF_{rel}^a)
	Control	γ -rays	I-SceI	γ -rays + I-SceI	
1	3.5	6.1	8,600	8,500	0.99
2	1.8	3.2	2,900	3,200	1.1
Mean	2.7	4.7	5,800	5,900	1.0 ($P = 0.82$) ^c

b) HR efficiency in TSCER2 cells

Exp.	TK ⁺ Revertant Frequency, RF ($\times 10^{-6}$)				Effect of IR (RF_{rel}^b)
	Control	γ -rays	I-SceI	γ -rays + I-SceI	
1	–	–	90	114	1.3
2	–	–	62	96	1.5
3	–	–	25	45	1.8
Mean	–	–	59	85	1.5 ($P = 0.021$) ^c

^a MF_{rel} was calculated as $MF(\gamma\text{-rays} + I\text{-SceI})/MF(I\text{-SceI})$

^b RF_{rel} was calculated as $RF(\gamma\text{-rays} + I\text{-SceI})/RF(I\text{-SceI})$

^c Assuming that they were paired data, P value was calculated by t -test

Table 2 Effect on DSB repair of exposure to 8.5 mGy IR at 0.125 mGy h⁻¹ following transfection with I-SceI expression vector (mode B)

Exp.	TK ⁻ Mutant Frequency, MF ($\times 10^{-6}$)				Effect of IR (MF_{rel}^a)
	Control	γ -rays	I-SceI	γ -rays + I-SceI	
1	2.8	1.3	3,400	4,500	1.3
2	3.1	2.8	12,000	17,000	1.4
3	–	–	11,000	11,000	1.0
Mean	3.0	2.1	8,800	10,800	1.2 ($P = 0.12$) ^c

b) HR efficiency in TSCER2 cells

Exp.	TK ⁺ Revertant Frequency, RF ($\times 10^{-6}$)				Effect of IR (RF_{rel}^b)
	Control	γ -rays	I-SceI	γ -rays + I-SceI	
1	–	–	82	160	2.0
2	–	–	160	270	1.7
3	–	–	110	190	1.7
Mean	–	–	120	210	1.8 ($P = 0.0013$) ^c

^a MF_{rel} was calculated as $MF(\gamma\text{-rays} + I\text{-SceI})/MF(I\text{-SceI})$

^b RF_{rel} was calculated as $RF(\gamma\text{-rays} + I\text{-SceI})/RF(I\text{-SceI})$

^c Assuming that they were paired data, P value was calculated by t -test

HR repair of DSBs by 50%. This 50% increase was found to be statistically significant by t -test ($P = 0.021$, if taken as paired data).

Effect of radiation exposure after I-SceI transfection on DSB repair (Mode B)

In the mode B experiment, the γ -irradiation was performed after transfection with the I-SceI vector to estimate the post-IR exposure effects on DSB repair. The mean MF_{rel} in TSCE5 cells exposed to IR following transfection was 1.2 (Table 2a) and the difference between unirradiated and irradiated cells was not statistically significant, indicating that post-transfection γ -irradiation had hardly any effect on NHEJ repair of DSBs. The mean RF_{rel} in TSCER2 cells under the same conditions, however, was 1.8 (Table 2b), indicating that exposure to γ -irradiation following transfection with I-SceI enhanced the HR repair of DSBs by 80%. This 80% increase was also found to be statistically significant by *t*-test ($P = 0.0013$, if taken as paired data).

Discussion

The efficiency of transfection using the amaxa nucleofection system was estimated to be about 40-fold higher than that using BioRad electroporation system, and this higher efficiency enabled us to more accurately estimate the repair of a single DSB at the specific I-SceI recognition site. As in our previous studies [4, 5], we observed that the frequencies of TK^+ revertants after the I-SceI vector transfection were lower than those of TK^- mutants. That finding seems to be consistent with the notion that NHEJ is the major repair pathway in mammalian cells [9]. Because our I-SceI system does not cover all NHEJ and HR events, it is however difficult to estimate the extent of DSB repair by HR. For example, our system does not cover sister-chromatid HR, which is probably the major HR pathway in mammalian cells. Small gene conversion events, not expanding to the exon 5 region, also cannot be detected by this system. Furthermore, there might be unknown factors, specific to this I-SceI site, which reduce the occurrences of the gene conversion type of events. Although the I-SceI system might over-estimate the repair efficiency of NHEJ compared with HR, it is a good model for elucidating the DSB repair associated with low-dose IR exposure.

Although transfection efficiencies varied from experiment to experiment, the relative TK^- mutant frequency and TK^+ revertant frequency were sufficient for evaluating the influence of IR on DSB repair. Both modes (A and B) of delivering low-dose, low dose-rate γ -irradiation were found to hardly influence NHEJ at the I-SceI site. Since an adaptive mutagenic response, a reduction of TK^- mutation frequency, was observed in TK6 cells exposed to X-rays (5 cGy of priming dose and 2 Gy of challenge dose) [10], we also measured DSB repair in cells in which the challenging X-ray exposure was replaced by I-SceI digestion.

In those measurements, similarly, NHEJ was barely influenced by the priming X-ray radiation (unpublished data), suggesting that an acute low-dose IR exposure also might provide the same tendency of “no influence” as that observed with the low-dose, low-dose-rate γ -irradiation. In contrast to NHEJ, both modes of γ -irradiation in the present experiments were found to considerably enhance HR at the I-SceI sites. This enhanced HR was not due to radiation-induced S/G2 arrest, because the low-dose IR did not affect the cell cycle (data not shown). Similar results were obtained when using a priming X-radiation (5 cGy; unpublished data).

The above similarities suggest that the enhancement of HR repair observed in the present study is a manifestation of an adaptive response where the low-dose, low-dose-rate γ -irradiation was the priming exposure. The inefficient effect of γ -irradiation on NHEJ does not seem to be consistent with a higher efficiency of DSB repair in radioadapted cells [11], as was shown by the reduction of genetic alterations at the chromosome level [12–14]. Since IR-induced DSBs were the major targets for adaptation in those studies, their DSBs might differ in some way from the I-SceI-induced DSBs we report on here. In other words, the fate of site-specific I-SceI breaks might reflect repair of spontaneous DSBs more faithfully than that of DSBs induced directly by relatively high dose exposure. At the present stage, it is very difficult to speculate plausible mechanisms responsible for the apparent adaptive response of DSB repair. We believe that the characteristics of I-SceI breaks and their continuous generation after the transfection are related to the observed repair characteristics. The enhanced repair by HR upon low-dose, low-dose-rate γ -irradiation is obviously not due to an enhanced cleavage of the I-SceI site after irradiation, since we have not observed such enhanced repair by NHEJ.

It remains to be tested whether NHEJ is really not enhanced by low-dose, low-dose-rate IR or whether it apparently remained stable because of limitations of the methodology. Recently, the fates of I-SceI breaks located in TSCE5 cells were determined in randomly isolated clones using non-phenotypic selection [5]. About 97% of the clones showed perfect rejoining, and deletions corresponding to the events detectable by the present selection method (i.e. large enough to affect the adjacent exon) were found in only 0.54% of the clones. Thus, if perfect NHEJ events or small deletion events were enhanced by low-dose, low-dose-rate γ -irradiation, we would not detect them by the present methodology.

In addition, the mechanisms responsible for HR repair, which is active in S/G2 phase cells, remains to be elucidated. In our previous studies using genetic analyses, we observed small homozygous LOH events in primed cells in the X-ray plus X-ray radioadaptive experiment mentioned

above [10]. We observed the same pattern of LOH mutants after low-dose, low-dose-rate γ -ray exposures [3], although the frequency was low. These results can be explained by the enhanced contribution of HR observed in the I-SceI digestion system, because this system could recover the non-crossing over gene conversion events very efficiently among the TK⁺ revertants. In near future we need to elucidate HR pathway leading to gene conversion, where a central core of protein, most likely the RecA homolog RAD51, plays a key role [15].

DSBs arise from endogenous sources including reactive oxygen species generated during cellular metabolisms. The DSB generation process mediated by reactive oxygen is suggested to be also involved in the indirect effects of the ionizing radiation exposure. As already described, the site-specific I-SceI break in our system can be considered as a good model for endogenous DSBs. Thus, enhanced HR repair activity induced by low-dose, low-dose-rate IR, might be regarded as defense machinery against DNA damage, whether occurring spontaneously and/or after low-dose, low-dose rate IR. At present, we are making an effort to apply the I-SceI digestion system for estimating DSB repair in bystander cells.

Acknowledgments This study was partially supported by the Budget for Nuclear Research of the Ministry of Education, Culture, Sports, Science and Technology, and was reviewed by the Atomic Energy Commission of Japan. We thank Dr. Miriam Bloom (SciWrite Biomedical Writing & Editing Services) for professional editing.

References

- Morimoto S, Kato T, Honma M, Hayashi M, Hanaoka F, Yatagai F (2002) Detection of genetic alterations induced by low-dose X rays: analysis of loss of heterozygosity for TK mutation in human lymphoblastoid cells. *Radiat Res* 157:533–538
- Morimoto S, Honma M, Yatagai F (2002) Sensitive detection of LOH events in a human cell line after C-ion beam exposure. *J Radiat Res* 43(Suppl):S163–S167
- Umebayashi Y, Honma M, Suzuki M, Suzuki H, Shimazu T, Ishioka N, Iwaki M, Yatagai F (2006) Mutation induction in cultured human cells after low-dose and low-dose-rate γ -ray irradiation: detection by LOH analysis. *J Radiat Res* 48:7–11
- Honma M, Izumi M, Sakuraba M, Tadokoro S, Sakamoto H, Wang W, Yatagai F, Hayashi M (2003) Deletion, rearrangement, and gene conversion; genetic consequences of chromosomal double-strand breaks in human cells. *Environ Mol Mutagen* 42:288–298
- Honma M, Sakuraba M, Koizumi T, Takashima T, Sakamoto H, Hayashi M (2007) Non-homologous end-joining for repairing I-SceI induced DNA double strand breaks in human cells. *DNA Repair* 6:781–788
- Jackson SP (2002) Sensing and repairing DNA double-strand breaks. *Carcinogenesis* 23:687–696
- Valerie K, Povirk LF (2003) Regulation and mechanisms of mammalian double-strand break repair. *Oncogene* 22:5792–5812
- Jeggo PA (1998) DNA breakage and repair. *Adv Genet* 38:185–282
- Pastwa E, Blasiak J (2003) Non-homologous end-joining. *Acta Biochim Pol* 50:891–908
- Yatagai F, Umebayashi Y, Honma M, Sugawara K, Takayama Y, Hanaoka F (2007) Mutagenic radioadaptation in a human lymphoblastoid cell line. *Mutat Res* 638:48–55
- Ikushima T, Aritomi H, Morisita J (1996) Radioadaptive response: efficient repair of radiation-induced DNA damage in adapted cells. *Mutat Res* 358:193–198
- Rigaud O, Papadopoulou D, Moustacchi E (1993) Decreased deletion mutation in radioadapted human lymphoblast. *Radiat Res* 133:94–101
- Azzam EL, Raaphorst GP, Mitchel RE (1994) Radiation-induced adaptive response for protection against micronucleus formation and neoplastic transformation in C3H 10T1/2 mouse embryo cells. *Radiat Res* 138:S28–S31
- Ueno AM, Vannais DB, Gustafson SL, Wong JC, Waldren CA (1996) A low adaptive dose of gamma-rays reduced the number and altered the spectrum of S1 mutants in human hamster hybrid cells. *Mutat Res* 358:161–169
- Li X, Heyer W-D (2008) Homologous recombination in DNA repair and DNA damage tolerance. *Cell Res* 18:99–113

ファルマシア

別刷

遺伝毒性物質に閾値はあるのか？

本間正充

Masamitsu HONMA

国立医薬品食品衛生研究所変異遺伝部室長

1 はじめに

食品の安全性に対して多くの国民が関心を寄せている今日、残留農薬や食品添加物等の食品中に含まれる微量の化学物質の安全性が問題となっている。多くの化学物質の毒性は、健康リスクを評価する場合、理論的、実証的研究から、これ以下であれば健康影響がみられないレベル、すなわち閾値がある用量反応モデルが用いられてきた。これにより1日摂取許容量(acceptable daily intake; ADI)を定めることができる。しかしながら、その化学物質の発がん性が問題となり、さらに遺伝毒性が認められるとやっかいである。他の毒性と異なり遺伝毒性には閾値がないとされているため、摂取量をゼロにしない限り健康リスクもゼロにならないとの論理からADIを設定することができない。ここに遺伝毒性発がん物質のリスク管理の問題点がある。

2 遺伝毒性とは？

遺伝毒性(genotoxicity)は遺伝子の本体であるDNAや染色体に対する毒性である。その定義は曖昧かつ広義であるが、一般には「DNAや染色体の構造的、もしくは量的変化を引き起こす性質」をいう。別の言葉として変異原性(mutagenicity)があるが、こちらは遺伝毒性に比べて狭義であり、主としてDNAや染色体に対する損傷の結果として生じる突然変異等の誘発能を示す(図1)。変異原性が最終的な遺伝的影響を示すものであり、それ以外の遺伝毒性はDNAや染色体が何らかの影響を受けたことによる一過性の変化であることが多い。遺伝毒性は他の毒性と異なり、それ自体の毒性の実態をつかむことができない。肝毒性、神経毒性、発がん性などは症状や病変として我々の体で認識できるが、遺伝毒性自体の症状や病変はない。

遺伝毒性はその結果として、がんや遺伝性疾患を引き起こす。したがって遺伝毒性とは、それら疾患を引き起こすポテンシャルの1つであり、その有無は遺伝毒性試験によって認識される。図1に一般的な遺伝毒性試験を示す。遺伝子DNAはバクテリアからは乳類まで共通する生命の設計図であり、様々な動物種を用いた試験法が開発されている。また、そのエンドポイントはDNAの損傷、染色体の構造的、もしくは数的変化、遺伝子突然変異等、多岐にわたる。このなかで代表的な試験法としてはエームス試験、染色体異常試験、小核試験(*in vivo*)が挙げられる。これら試験は医薬品を初めとする多くの化学物質の安全性を評価する上で必須の試験として義務づけられている。

遺伝毒性試験は一般的に、遺伝毒性ハザードの有無を検出する定性的試験法であり、その結果は「陽性」もしくは「陰性」として判定される。しかしながら、毒性には本来、量的相関性

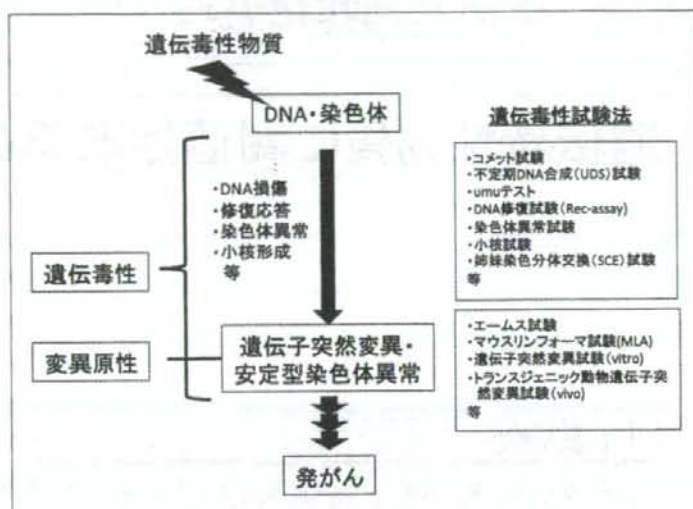


図1 遺伝毒性とその試験法

があることが常識であり、遺伝毒性のような一義的に陽性、陰性を決定することの方が特殊といえる。したがって、遺伝毒性の閾値問題はこの結果の定性的評価法に端を発するといえよう。最近になってトランスジェニック動物の開発等によって遺伝子突然変異試験等の定量的試験法が *in vivo* で実用可能となった。また、遺伝子突然変異はがんを引き起こす直接要因であることから、その試験結果は発がん性遺伝毒性物質評価の重要なエビデンスにもなりうる。

3 遺伝毒性発がん物質、非遺伝毒性発がん物質

遺伝毒性試験の目的の1つは、化学物質等の発がん可能性を調査するためのスクリーニングである。しかし、遺伝毒性試験で陽性となったからといって必ずしも発がん性があるとは限らない。遺伝毒性試験結果とげっ歯類発がん性試験結果の相関性は、試験系によっても異なるが60~80%程度である。スクリーニングとしての目的上、できるだけ多くの発がん可能性を検出することが求められるため、感度の高い試験法が開発・利用されてきたが、それでも一部の発がん性物質に関しては陰性を示す。これらが非遺伝毒性発がん物質である。がんは遺伝子の病気であり、必ず遺伝的な変化を伴うと考えられるが、これらの物質は自然に生じたがん原細胞の増殖の亢進などを通じてがんの形成を助けるものと考えられる。ホルモン作用を持つ化学物質の一部などがこれに相当する。

遺伝毒性物質にはベンツピレン、アフラトキシン B1、N-ニトロソ化合物、アルキル化剤などの強力な発がん物質が含まれる。これら化学物質はDNAに直接作用し、切断、架橋、付加体の形成、脱塩基、酸化損傷、アルキル化等を引き起こし、その結果、高い確率で突然変異を引き起こす。一方、遺伝毒性試験で陽性であっても直接DNAに作用しないものもある。チューブリンの重合阻害剤であるコルヒチンは細胞分裂装置に影響を与え、染色体異常を引き起こす。また、DNA修復阻害、アポトーシス抑制、細胞周期停止などを引き起こす化学物質も遺伝毒性試験で陽性を示すことがある。

これら、化学物質のターゲットはDNAではなくタンパク質であり、非DNA損傷性遺伝毒